Using Frequency-Response Functions to Investigate String Stability of Cooperative Control Laws

Lesley A. Weitz*
The MITRE Corporation, McLean, VA, 22102, U.S.A
John E. Hurtado†
Texas A&M University, College Station, TX, 77843, U.S.A.

Decentralized, cooperative control laws couple separate vehicles in order to achieve a common objective. In this paper, the development of cooperative control laws for multivehicle formations is presented. The closed-loop equations of motion for the multivehicle system are shown to be analogous to structural systems, and the stability and performance of the system can be investigated using frequency-response functions. The main contribution of the paper is an alternate approach to evaluate string stability of cooperative control laws using a frequency-response framework. Simulation results for four different cooperative-control forms are presented, and the string-stability results are evaluated and discussed.

I. Introduction

Advances in communication, navigation, and computational systems have enabled greater autonomy in multivehicle systems. These technological advances have resulted in a paradigm shift toward decentralized, cooperative systems where control inputs are determined at the individual vehicle level using state and environmental information. Decentralized, cooperative control applications include autonomous spacing of aircraft in next-generation air traffic systems[1,2] and UAV/MAV formation control.[3,4,5]

Decentralized systems refer to distributed processing across many nodes or vehicles, and this approach can be more computationally efficient than centralized systems, wherein processing is commonly performed at a single node. Cooperative control laws for multivehicle systems couple the otherwise separate vehicle dynamics (or governing equations) via shared state information in order to achieve a common objective. Control-law design is largely based on a desired communication structure that defines the information available to each vehicle in the system. Communication structures may be constrained by sensing, communication, or computational limitations. For example, in many applications, vehicles only communicate with their "nearest neighbors" rather than all vehicles in the system. In the past, researchers have investigated the effects of communication structures, or information flow, on system stability using graph theory.[3,6,7,8]

Two stability concepts that arise in the design of decentralized, cooperative control laws for formation control are internal stability and string stability. Internal stability investigates whether spacing errors between vehicle pairs go to zero and the multivehicle system reaches a desired formation in the absence of disturbances.[4] String stability deals with how errors are propagated through the vehicle string due to disturbances or the reference trajectory of the formation lead.[9] A string-stable control form implies that spacing errors between adjacent vehicles are not amplified along the vehicle string. The concept of string stability has been extensively studied for automated highway systems where vehicle strings of infinite length are considered.[9,10,11,12,13] That research showed that the communication structure has a direct effect on string stability. For example, it was shown that a vehicle system is string unstable if information is passed from the immediately preceding vehicle only.[9]

In this paper, closed-loop equations of motion for the multivehicle system are written in a structural form, where the form of the stiffness and damping matrices is determined by the assumed communication structure.

*Senior Simulation and Modeling Engineer, 7515 Colshire Drive, and AIAA Member.
†Associate Professor, 3141 TAMU, and AIAA Senior Member.

Motivated by the analogy of cooperative multivehicle systems to structural systems, the disturbance-rejection and string-stability properties of different cooperative control forms are explored using frequency-response functions. For the vehicle model used here, disturbances act at the kinematic level. Frequency-response information is used to determine how disturbance effects impact the multivehicle system, and more specifically, how disturbances are propagated through the formation. Steady-state solutions, derived from the frequency response, of the disturbed system are used to determine string stability, and these results can be used to compare different communication structures.

The main contribution of this paper is the development of a mechanics-based approach to analyze the disturbance-rejection and string-stability properties of general cooperative control forms, which are derived from communication structures. This approach allows the disturbance-rejection and string-stability properties of different communication structures to be evaluated using a common framework. Although the form of the disturbances presented here is specific to how disturbances affect the chosen vehicle model, this approach to analyzing disturbance rejection and string stability can be easily modified to fit a desired application. Therefore, the analysis presented can be applied to other cooperative control applications that are analogous to structural systems.

The organization of the paper is as follows. In Section II, the assumed vehicle model and the development of the cooperative control laws are described. The structural analogy is presented in Section III. The disturbed vehicle model, frequency-response functions for multi-degree-of-freedom (MDOF) systems, and the steady-state solutions used to determine string stability are discussed in Section IV. In Section V, simulation results are presented for four different communication structures. Lastly, conclusions are presented in Section VI.

II. Development of the Cooperative Control Laws

As described previously, cooperative control laws can be designed to drive errors between vehicles to zero to achieve a desired formation. This section describes a unifying approach to the design of cooperative control laws using the communication-structure concept. A nonlinear model for planar vehicle motion is discussed, the error variables and control inputs are presented, and lastly, the analogy of the closed-loop system to structural systems is shown.

A. Vehicle Model

The development of the cooperative control laws presented here is based upon a commonly-used nonlinear vehicle model. This model represents vehicles with negligible velocity in the direction perpendicular to the vehicle's heading and can be used to represent the planar motion of UAVs.

$$\dot{x} = v\cos\theta; \qquad \dot{y} = v\sin\theta; \qquad \dot{\theta} = \omega \tag{1}$$

Here, x and y are the inertial position of the vehicle, and θ is the heading angle with respect to the x axis. The control inputs to the vehicle are the velocity, v, and angular turn rate, ω.

This vehicle model is differentially flat with flat outputs x and y, which allows the vehicle states and controls to be expressed as functions of the flat outputs and their higher derivatives.[5,14]

$$\theta = \tan^{-1}\left(\frac{\dot{y}}{\dot{x}}\right); \qquad v = \sqrt{\dot{x}^2+\dot{y}^2}; \qquad \omega = \frac{\ddot{y}\dot{x}-\dot{y}\ddot{x}}{v^2} \tag{2}$$

Second derivatives of the flat outputs are the highest derivatives that appear in ω, and a time derivative of the velocity reveals the second derivatives of the flat outputs.

$$\dot{v} = \frac{\dot{x}\ddot{x}+\dot{y}\ddot{y}}{v} \tag{3}$$

Therefore, new control inputs can be defined as $(\ddot{x},\ddot{y}) = (u,w)$, and the nonlinear system in Equation (1) can be represented as uncoupled double integrators.

The differentially-flat system enables control design in the flat-output (x,y) space, and these control inputs are then mapped to the vehicle inputs $\dot{v}$ and ω using the linear transformation.

$$\begin{bmatrix}\dot{v}\\ \omega\end{bmatrix} = \frac{1}{v}\begin{bmatrix}\dot{x} & \dot{y}\\ -\frac{\dot{y}}{v} & \frac{\dot{x}}{v}\end{bmatrix}\begin{bmatrix}u\\ w\end{bmatrix} = T\left(\dot{x},\dot{y}\right)\begin{bmatrix}u\\ w\end{bmatrix}; \qquad v = \sqrt{\dot{x}^2+\dot{y}^2} \tag{4}$$

B. Definition of Spacing Errors

The cooperative control laws developed here are functions of spacing errors between vehicles. The number of error terms in an n-vehicle system is $n_e = \left(\sum_{j=1}^{n-1} j\right) + 1$. For example, in a three-vehicle formation as shown in Figure 1, there are four error terms.

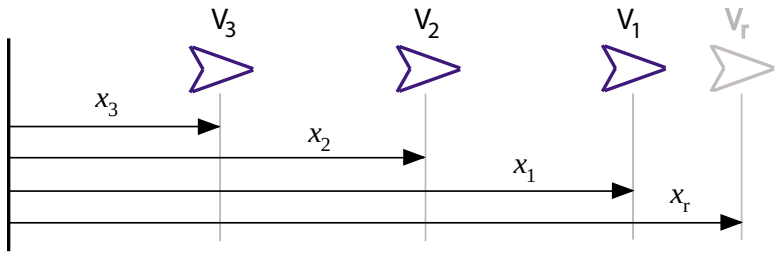

Figure 1. Example of a three-vehicle formation.

The development is shown in the x direction only (the development in the y direction is identical).

$$\begin{aligned}
e_{r1} &= x_r - x_1 - d_{r1}; \quad \dot{e}_{r1} = \dot{x}_r - \dot{x}_1; \quad \ddot{e}_{r1} = -u_1 \\
e_{12} &= x_1 - x_2 - d_{12}; \quad \dot{e}_{12} = \dot{x}_1 - \dot{x}_2; \quad \ddot{e}_{12} = u_1 - u_2 \\
e_{13} &= x_1 - x_3 - d_{13}; \quad \dot{e}_{13} = \dot{x}_1 - \dot{x}_3; \quad \ddot{e}_{13} = u_1 - u_3 \\
e_{23} &= x_2 - x_3 - d_{23}; \quad \dot{e}_{23} = \dot{x}_2 - \dot{x}_3; \quad \ddot{e}_{23} = u_2 - u_3
\end{aligned} \tag{5}$$

Here, x_r denotes a defined reference trajectory that the first vehicle tracks, and it is assumed that x_r is a constant-velocity trajectory. The constants, d_{r1}, d_{12}, d_{13}, and d_{23}, denote the desired distances between vehicles. Note that there are r equations that constrain the error terms, where $r = n_e - n$. In a three-vehicle formation, there is one constraint equation $e_{13} = e_{12} + e_{23}$, and equivalently, $d_{13} = d_{12} + d_{23}$.

C. Cooperative Control Laws

Control inputs are functions of the spacing errors as defined by the selected communication structure. For example, in a fully-connected system where all vehicles have information about all other vehicles in the formation, the control inputs have the following form.

$$\begin{aligned}
u_1 &= -k_{12}e_{12} - c_{12}\dot{e}_{12} - k_{13}e_{13} - c_{13}\dot{e}_{13} + k_{r1}e_{r1} + c_{r1}\dot{e}_{r1} \\
u_2 &= k_{12}e_{12} + c_{12}\dot{e}_{12} - k_{23}e_{23} - c_{23}\dot{e}_{23} \\
u_3 &= k_{13}e_{13} + c_{13}\dot{e}_{13} + k_{23}e_{23} + c_{23}\dot{e}_{23}
\end{aligned} \tag{6}$$

It is assumed that the control gain k_{ij} (c_{ij}) on the spacing error e_{ij} ($\dot{e}_{ij}$) is the same wherever it is used. This assumption reduces some of the design degrees of freedom and is done for simplicity; it is not a necessary constraint.

The closed-loop error dynamics can be written in a second-order form by substituting the control inputs into the second derivatives of the error terms ($\ddot{e}_{r1}$, $\ddot{e}_{12}$, and $\ddot{e}_{23}$) and using the constraint equation $e_{13} = e_{12} + e_{23}$. The error dynamics are homogeneous and stable for control gains greater than zero, which indicates that spacing errors will asymptotically converge to zero.

III. Structural Analogy

The closed-loop equations of motion for the multivehicle system are analogous to physically-connected systems or structures, where individual mass elements are connected by springs and dampers. The closed-loop system can be written in a structural form.

$$M\ddot{\boldsymbol{x}} + C\dot{\boldsymbol{x}} + K\boldsymbol{x} = D\boldsymbol{u_r} \tag{7}$$

Here, $\boldsymbol{x}$ is an $n \times 1$ vector of vehicle positions, and M, C, and K are $n \times n$ matrices. The matrix M is the mass matrix, which is equal to identity; C is the damping matrix; and, K is the stiffness matrix. The term on the right-hand side of Equation (7) is a forcing term related to the reference trajectory and the constant desired distances between vehicles. For example, the stiffness matrix and forcing terms can be found using the control inputs in Equation (6). The damping matrix has the same form and is proportional to the stiffness matrix.

$$K = \begin{bmatrix} k_{r1} + k_{12} + k_{13} & -k_{12} & -k_{13} \\ -k_{12} & k_{12} + k_{23} & -k_{23} \\ -k_{13} & -k_{23} & k_{13} + k_{23} \end{bmatrix} \tag{8}$$

$$D = \begin{bmatrix} k_r & c_r & -k_{r1} & k_{12} & k_{13} & 0 \\ 0 & 0 & 0 & -k_{12} & 0 & k_{23} \\ 0 & 0 & 0 & 0 & -k_{13} & -k_{23} \end{bmatrix}; \quad \boldsymbol{u_r} = \begin{bmatrix} x_r(t) & \dot{x}_r(t) & d_{r1} & d_{12} & d_{13} & d_{23} \end{bmatrix}^T \tag{9}$$

The form of the stiffness matrix is related to the assumed communication structure for the system. Thus, different communication structures will yield different stiffness matrices. Whereas all closed-loop equations of motion can be written in the structural form in Equation (7), not all communication structures yield a physical representation. Here, the structural analogy refers to the ability to write the closed-loop equations of motion in the linear structural form, rather than an analogy to true physical systems.

Other researchers have noted the connection between communication structures and structural systems; however, this relationship has been treated literally in that the closed-loop equations of motion can be physically represented by masses connected by springs and dampers.[8] In contrast, the Laplacian matrix used by Fax and Murray is directed and therefore does not necessarily yield a physical representation;[3] similar to that work, the communication structures in this research are not constrained to be physically representative. This is further explained in Section V.

IV. Frequency-Response Functions and String Stability

Some communication structures may demonstrate better disturbance rejection than others; i.e., some communication structures may yield string-stable control laws, whereas others may yield string-unstable control laws. In this section, the disturbed vehicle model is presented, and a frequency-response approach for analyzing single-degree-of-freedom (SDOF) and MDOF systems is reviewed. The steady-state solutions are developed for the MDOF systems, and the analogy to string stability is discussed.

A. Vehicle Model with Disturbances

The form of the disturbances in the original nonlinear vehicle model is first related to the transformation that describes the vehicle in the double-integrator design space, which has motivated the theoretical developments to this point. The nonlinear vehicle model in Equation (1) represents vehicles with no sideslip, and the transformation to the double-integrator representation enforces the nonholonomic or kinematic constraint. Disturbances to the nonlinear model, of the form shown below, can be considered disturbances to the kinematic constraint.

$$\begin{aligned} \dot{x} &= v\cos\theta + d_x \\ \dot{y} &= v\sin\theta + d_y \\ \dot{\theta} &= \omega \end{aligned} \tag{10}$$

The disturbed vehicle model requires some definition of terms. The velocity v is the ideal velocity, or the commanded velocity of the vehicle, which can be measured using onboard sensors, and the angle θ is the true heading angle of the vehicle. The $v\cos\theta$ and $v\sin\theta$ terms are the projections of the ideal velocities in the x and y directions, and may be denoted as v_x and v_y, respectively. The sum of the projections of the ideal velocities and the disturbance terms, $\dot{x}$ and $\dot{y}$, are the true velocities in the x and y directions, respectively.

The disturbance velocity has magnitude v_d and angle ψ with respect to the horizontal axis.

$$v_d = \sqrt{\dot{x}^2 + \dot{y}^2} = \sqrt{(v_x + d_x)^2 + (v_y + d_y)^2} \tag{11}$$

$$\psi = \tan^{-1}\left(\frac{\dot{y}}{\dot{x}}\right) = \tan^{-1}\left(\frac{v_y + d_y}{v_x + d_x}\right) \tag{12}$$

The sideslip angle is the difference between the angle of the disturbance velocity and the true vehicle heading: $\beta = \psi - \theta$. These quantities are illustrated in Figure 2.

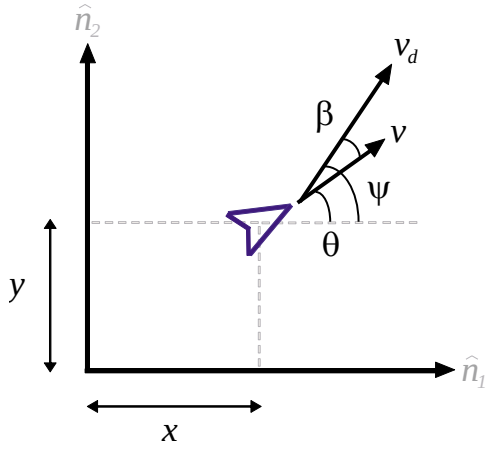

Figure 2. Disturbed vehicle model.

The ideal velocity and the true heading angle can also be written as a function of the true velocities and the disturbances.

$$v = \sqrt{(\dot{x} - d_x)^2 + (\dot{y} - d_y)^2}; \qquad \theta = \tan^{-1}\left(\frac{\dot{y} - d_y}{\dot{x} - d_x}\right) \tag{13}$$

The vehicle controls, $\dot{v}$ and ω, are found by taking derivatives of the above expressions.

$$\dot{v} = \frac{(\dot{x} - d_x)(\ddot{x} - \dot{d}_x) + (\dot{y} - d_y)(\ddot{y} - \dot{d}_y)}{v} \tag{14}$$

$$\omega = \frac{(\dot{x} - d_x)(\ddot{y} - \dot{d}_y) - (\dot{y} - d_y)(\ddot{x} - \dot{d}_x)}{v^2} \tag{15}$$

If the disturbances (d_x, $\dot{d}_x$, d_y, and $\dot{d}_y$) are known, then the controls can be chosen as $\ddot{x} = u(x, \dot{x})$ and $\ddot{y} = w(y, \dot{y})$. In other words, if one can determine the true velocities from knowledge of d_x and d_y, then the controls are functions of positions and true velocities. The transformation to $\dot{v}$ and ω becomes a function of disturbance rates.

$$\begin{bmatrix} \dot{v} \\ \omega \end{bmatrix} = \frac{1}{v}\begin{bmatrix} v_x & v_y \\ -\frac{v_y}{v} & \frac{v_x}{v} \end{bmatrix}\begin{bmatrix} u - \dot{d}_x \\ w - \dot{d}_y \end{bmatrix} \tag{16}$$

This transformation essentially cancels the effects of the disturbances by controlling the true accelerations of the vehicle and subtracting the disturbance rates.

If the disturbances are unknown, then the controls can be chosen as $\dot{v}_x = u(x, v_x)$ and $\dot{v}_y = w(y, v_y)$. Therefore, the controls are calculated using knowledge of the ideal velocity and true heading angle only. In this case, the controls and transformation are not functions of the disturbances, and the transformation looks the same as when no disturbances are present.

$$\begin{bmatrix} \dot{v} \\ \omega \end{bmatrix} = \frac{1}{v}\begin{bmatrix} v_x & v_y \\ -\frac{v_y}{v} & \frac{v_x}{v} \end{bmatrix}\begin{bmatrix} u \\ w \end{bmatrix} \tag{17}$$

The disturbed vehicle model in Equation (10) is still expressed as double integrators that are decoupled

in the x and y directions. The disturbances act at the kinematic level in the double-integrator form.

Known Disturbance:	$\dot{x} = v_x + d_x$	$\dot{y} = v_y + d_y$
	$\ddot{x} = u(x, \dot{x})$	$\ddot{y} = w(y, \dot{y})$
Unknown Disturbance:	$\dot{x} = v_x + d_x$	$\dot{y} = v_y + d_y$
	$\dot{v}_x = u(x, v_x)$	$\dot{v}_y = w(y, v_y)$

As in Section II, control inputs are designed using the double-integrator form, and the vehicle controls are determined using the appropriate transformation. This paper deals with the case that the disturbances are unknown and cannot be canceled by the transformation.

B. Frequency-Response Functions

Frequency-response functions (FRFs) describe the steady-state response of a system to harmonic excitation for a given input frequency.[15,16] For SDOF systems, the FRF can be used to design controllers and select control gains to stabilize an open-loop system. A closed-loop FRF provides information about a system's ability to track low-frequency signals and reject high-frequency noise. Here, the MDOF FRFs are used to evaluate disturbance effects on the multivehicle system.

1. *SDOF Systems*

Consider a scalar, second-order system subject to harmonic excitation with amplitude f.

$$m\ddot{x} + c\dot{x} + kx = f\cos(\sigma t) \tag{18}$$

The system in Equation (18) has a steady-state solution of the form $x_{ss} = X\cos(\sigma t - \alpha)$, where X is the output amplitude and α is the phase shift. The FRF is composed of two parts: the ratio of the steady-state amplitude to the static response, $H(\sigma)$, and the phase of the response, α.[15]

$$H(\sigma) = \frac{X}{x_{static}} = \frac{k}{\sqrt{(k^2 - m\sigma^2)^2 + (c\sigma)^2}}; \qquad \alpha = \tan^{-1}\left(\frac{c\sigma}{k^2 - m\sigma^2}\right) \tag{19}$$

Equation 19 can also be written in terms of the natural frequency and damping ratio, $\omega^2 = k/m$ and $2\zeta\omega = c/m$, and the ratio of the excitation frequency to the natural frequency, $r = \sigma/\omega$.

$$H(r) = \frac{1}{\sqrt{(1 - r^2)^2 + (2\zeta r)^2}}; \qquad \alpha = \tan^{-1}\left(\frac{2\zeta r}{1 - r^2}\right) \tag{20}$$

Of greater interest in this case is the receptance function, which is the ratio of the steady-state amplitude to the excitation amplitude.

$$\frac{X}{f} = \frac{1}{\sqrt{(\omega^2 - \sigma^2)^2 + (2\zeta\omega\sigma)^2}} \tag{21}$$

In the case of a disturbance input, Equation (21) determines the amplification of the disturbance by the system.

2. *MDOF Systems*

System receptance functions for MDOF systems relate steady-state amplitudes of the jth output to the kth input. The MDOF receptance functions are determined using modal coordinates[17] and appropriate transformations to express ratios in terms of physical coordinates. The structural system in Equation (7) is expressed in the familiar first-order form with disturbances acting at the kinematic level. The forcing terms on the right-hand side of Equation (7) are assumed equal to zero for the frequency-response analysis.

$$\dot{\boldsymbol{z}} = \left[\begin{array}{c:c} 0 & I \\ \hdashline -M^{-1}K & -M^{-1}C \end{array}\right]\boldsymbol{z} + \left[\begin{array}{c} \boldsymbol{f}\cos(\sigma t) \\ \hdashline 0 \end{array}\right]; \qquad \boldsymbol{z} = \left[\begin{array}{c} \boldsymbol{x} \\ \hdashline \boldsymbol{v_x} \end{array}\right] \tag{22}$$

Note that the control, which is represented by the lower partition of Equation (22), is a function of the position and ideal velocity because the disturbance is assumed unknown.

Equation (22) can be decoupled using a modal-coordinate transformation, where $\boldsymbol{x} = \Phi\boldsymbol{\eta_1}$ and $\boldsymbol{v_x} = \Phi\boldsymbol{\eta_2}$; $\boldsymbol{\eta_1}$ is an $n \times 1$ vector of modal positions, $\boldsymbol{\eta_2}$ is an $n \times 1$ vector of modal velocities, and Φ is the $n \times n$ matrix of eigenvectors of the stiffness matrix.[17]

$$\dot{\boldsymbol{z}}_{\boldsymbol{\eta}} = \left[\begin{array}{c|c} 0 & I \\ \hline -\tilde{K} & -\tilde{C} \end{array}\right] \boldsymbol{z}_{\boldsymbol{\eta}} + \left[\begin{array}{c} \tilde{\boldsymbol{f}}\cos(\sigma t) \\ \hline 0 \end{array}\right]; \qquad \boldsymbol{z}_{\boldsymbol{\eta}} = \left[\begin{array}{c} \boldsymbol{\eta_1} \\ \hline \boldsymbol{\eta_2} \end{array}\right] \tag{23}$$

Here, $\tilde{K} = \Phi^{-1}K\Phi$, $\tilde{C} = \Phi^{-1}C\Phi$, and $\tilde{\boldsymbol{f}} = \Phi^{-1}\boldsymbol{f}$. To diagonalize the equations of motion in Equation (7), and equivalently in Equation (23), the Φ matrix must have n linearly independent eigenvectors.

The ith mode can be described by the set of first-order equations.

$$\dot{\eta}_{i,1} = \eta_{i,2} + \tilde{f}_i \cos(\sigma t) \tag{24}$$

$$\dot{\eta}_{i,2} = -\tilde{K}_i\eta_{i,1} - \tilde{C}_i\eta_{i,2} \tag{25}$$

To be rigorous in terminology, $\dot{\eta}_{i,1}$ is the true modal velocity, and $\eta_{i,2}$ is the ideal modal velocity. A derivative is taken of Equation (24) and appropriate substitutions are made in order to write the equations of motion for the ith mode in a second-order form.

$$\begin{aligned} \ddot{\eta}_{i,1} &= \dot{\eta}_{i,2} - \sigma\tilde{f}\sin(\sigma t) \\ &= -\tilde{K}_i\eta_{i,1} - \tilde{C}_i\eta_{i,2} - \sigma\tilde{f}\sin(\sigma t) \\ &= -\tilde{K}_i\eta_{i,1} - \tilde{C}_i\left(\dot{\eta}_{i,1} - \tilde{f}_i\cos(\sigma t)\right) - \sigma\tilde{f}_i\sin(\sigma t) \end{aligned} \tag{26}$$

Thus, the second-order equation that describes the ith modal dynamics subject to a kinematic disturbance has two excitation terms on the right-hand side.

$$\ddot{\eta}_{i,1} + \tilde{C}_i\dot{\eta}_{i,1} + \tilde{K}_i\eta_{i,1} = \tilde{C}_i\tilde{f}_i\cos(\sigma t) - \sigma\tilde{f}_i\sin(\sigma t) \tag{27}$$

The steady-state solution to the above expression can be written as a sum of the steady-state solutions for the $\cos(\cdot)$ and $\sin(\cdot)$ excitation terms.

$$\eta_{i,ss} = N_i^I\cos(\sigma t - \alpha_i^I) + N_i^{II}\sin(\sigma t - \alpha_i^{II}). \tag{28}$$

The receptance functions and phases for each term in the solution are found using the same approach for SDOF systems, where r_i is the ratio of the excitation frequency to the ith natural frequency.[15]

$$\frac{N_i^I}{\tilde{f}_i} = \frac{\tilde{C}_i}{\omega_i^2\sqrt{(1-r_i^2)^2 + (2\zeta_i r_i)^2}}; \qquad \alpha_i^I = \tan^{-1}\left(\frac{2\zeta_i\omega_i\sigma}{\omega_i^2 - \sigma^2}\right) \tag{29}$$

$$\frac{N_i^{II}}{\tilde{f}_i} = \frac{\sigma}{\omega_i^2\sqrt{(1-r_i^2)^2 + (2\zeta_i r_i)^2}}; \qquad \alpha_i^{II} = \tan^{-1}\left(\frac{-2\zeta_i\omega_i\sigma}{\sigma^2 - \omega_i^2}\right) \tag{30}$$

The steady-state amplitudes in modal coordinates are transformed to the steady-state amplitudes in physical coordinates using the modal matrix.

$$\boldsymbol{X} = \Phi(\boldsymbol{N}^I + \boldsymbol{N}^{II}) \tag{31}$$

The vectors of modal amplitudes are $\boldsymbol{N}^I = D^I\Phi^{-1}\boldsymbol{f}$ and $\boldsymbol{N}^{II} = D^{II}\Phi^{-1}\boldsymbol{f}$, where D^I and D^{II} are defined below.

$$D^I = \text{diag}\left(\frac{\tilde{C}_1}{\omega_1^2 s_1}, \frac{\tilde{C}_2}{\omega_2^2 s_2}, ..., \frac{\tilde{C}_n}{\omega_n^2 s_n}\right); \qquad D^{II} = \text{diag}\left(\frac{\sigma}{\omega_1^2 s_1}, \frac{\sigma}{\omega_2^2 s_2}, ..., \frac{\sigma}{\omega_n^2 s_n}\right) \tag{32}$$

The term s_i is the square root term in Equations (29) and (30): $s_i = \sqrt{(1-r_i^2)^2 + (2\zeta_i r_i)^2}$.

The receptance functions for the MDOF system in physical coordinates are determined via appropriate substitutions.

$$H_{jk} \equiv \frac{X_j}{f_k} = \left[\Phi(D^I + D^{II})\Phi^{-1}\right]_{jk} \tag{33}$$

Here, H is an $n \times n$ matrix, and the (j,k)th element of H is the ratio of the jth output to the kth input. More specifically for the multivehicle-control application, H_{jk} is the ratio of the jth vehicle's steady-state amplitude to the kth vehicle's disturbance amplitude, and thus, reveals the disturbance-rejection properties of the given cooperative-control form. The matrix H is symmetric if the eigenvector matrix Φ is symmetric, which is guaranteed if the stiffness matrix K is symmetric.

Whereas the receptance functions show the magnitudes of the steady-state responses relative to disturbance inputs from each vehicle, the steady-state amplitude of the jth vehicle reveals the cumulative effects of disturbances to all other vehicles in the formation. Steady-state amplitudes and steady-state errors are determined using both the steady-state modal amplitudes and the phase information.

C. Steady-State Solution from Frequency-Response Functions

Whereas the receptance function, H, shows how vehicles are affected by the disturbances to other vehicles, the steady-state solution is used to find the maximum steady-state amplitude of each vehicle as a function of σ. The steady-state response of the ith vehicle in physical coordinates can be expressed using the superposition of the modal-coordinate responses.

$$x_{i,ss}(t) = x^I_{i,ss}(t) + x^{II}_{i,ss}(t) = \Phi_{ij}\left[N^I_j \cos(\sigma t - \alpha^I_j) + N^{II}_j \sin(\sigma t - \alpha^{II}_j)\right] \tag{34}$$

The first term in Equation (34) can be expanded and rearranged.

$$\begin{aligned} x^I_{i,ss}(t) &= \Phi_{i1}N^I_1 \cos(\sigma t - \alpha^I_1) + \Phi_{i2}N^I_2 \cos(\sigma t - \alpha^I_2) + ... + \Phi_{in}N^I_n \cos(\sigma t - \alpha^I_n) \\ &= \Phi_{i1}N^I_1 \left[\cos(\sigma t)\cos(\alpha^I_1) + \sin(\sigma t)\sin(\alpha^I_1)\right] + \\ &\quad + \Phi_{i2}N^I_2 \left[\cos(\sigma t)\cos(\alpha^I_2) + \sin(\sigma t)\sin(\alpha^I_2)\right] + ... \\ &\quad ... + \Phi_{in}N^I_n \left[\cos(\sigma t)\cos(\alpha^I_n) + \sin(\sigma t)\sin(\alpha^I_n)\right] \\ &= \sin(\sigma t)\left[\Phi_{i1}N^I_1 \sin(\alpha^I_1) + \Phi_{i2}N^I_i \sin(\alpha^I_2) + ... + \Phi_{in}N^I_n \sin(\alpha^I_n)\right] + \\ &\quad + \cos(\sigma t)\left[\Phi_{i1}N^I_1 \cos(\alpha^I_1) + \Phi_{i2}N^I_i \cos(\alpha^I_2) + ... + \Phi_{in}N^I_n \cos(\alpha^I_n)\right] \end{aligned} \tag{35}$$

The response is written as $x^I_{i,ss}(t) = A_i \sin(\sigma t) + B_i \cos(\sigma t)$.

$$A_i = \Phi_{i1}N^I_1 \sin(\alpha^I_1) + \Phi_{i2}N^I_i \sin(\alpha^I_2) + ... + \Phi_{in}N^I_n \sin(\alpha^I_n) \tag{36}$$

$$B_i = \Phi_{i1}N^I_1 \cos(\alpha^I_1) + \Phi_{i2}N^I_i \cos(\alpha^I_2) + ... + \Phi_{in}N^I_n \cos(\alpha^I_n) \tag{37}$$

The second term in Equation (34) can be rearranged similarly.

$$\begin{aligned} x^{II}_{i,ss}(t) = \sin(\sigma t)&\left[\Phi_{i1}N^{II}_1 \cos(\alpha^{II}_1) + \Phi_{i2}N^{II}_2 \cos(\alpha^{II}_2) + ... + \Phi_{in}N^{II}_n \cos(\alpha^{II}_n)\right] - \\ &- \cos(\sigma t)\left[\Phi_{i1}N^{II}_1 \sin(\alpha^{II}_1) + \Phi_{i2}N^{II}_2 \sin(\alpha^{II}_2) + ... + \Phi_{in}N^{II}_n \sin(\alpha^{II}_n)\right] \end{aligned} \tag{38}$$

Here, $x^{II}_{i,ss}(t) = C_i \sin(\sigma t) - D_i \cos(\sigma t)$.

$$C_i = \Phi_{i1}N^{II}_1 \cos(\alpha^{II}_1) + \Phi_{i2}N^{II}_2 \cos(\alpha^{II}_2) + ... + \Phi_{in}N^{II}_n \cos(\alpha^{II}_n) \tag{39}$$

$$D_i = \Phi_{i1}N^{II}_1 \sin(\alpha^{II}_1) + \Phi_{i2}N^{II}_2 \sin(\alpha^{II}_2) + ... + \Phi_{in}N^{II}_n \sin(\alpha^{II}_n) \tag{40}$$

Therefore, the steady-state response of the ith vehicle is expressed as the sum of $x^I_{i,ss}(t)$ and $x^{II}_{i,ss}(t)$.

$$x_{i,ss}(t) = (A_i + C_i)\sin(\sigma t) + (B_i - D_i)\cos(\sigma t). \tag{41}$$

The amplitude of the steady-state solution is: $X_{i,ss} = \sqrt{(A_i + C_i)^2 + (B_i - D_i)^2}$. Vector expressions for A, B, C, and D are calculated using the following expressions.

$$\boldsymbol{A} = \Phi \ \mathrm{diag}(\boldsymbol{N}^I)\sin(\boldsymbol{\alpha}^I) \tag{42}$$

$$\boldsymbol{B} = \Phi \ \mathrm{diag}(\boldsymbol{N}^I)\cos(\boldsymbol{\alpha}^I) \tag{43}$$

$$\boldsymbol{C} = \Phi \ \mathrm{diag}(\boldsymbol{N}^{II})\cos(\boldsymbol{\alpha}^{II}) \tag{44}$$

$$\boldsymbol{D} = \Phi \ \mathrm{diag}(\boldsymbol{N}^{II})\sin(\boldsymbol{\alpha}^{II}) \tag{45}$$

The steady-state error between adjacent vehicles is easily found using the steady-state solutions.

$$e_{(i-1,i),ss}(t) = (A_{i-1} + C_{i-1} - A_i - C_i)\sin(\sigma t) + (B_{i-1} - D_{i-1} - B_i + D_i)\cos(\sigma t) \tag{46}$$

Therefore, the amplitude of the steady-state error is:

$$E_{(i-1,i),ss} = \sqrt{(A_{i-1} + C_{i-1} - A_i - C_i)^2 + (B_{i-1} - D_{i-1} - B_i + D_i)^2}. \tag{47}$$

D. Interpretation of the Frequency-Response Analysis

Frequency-response analysis is typically used to investigate the natural frequencies and modes of structural systems, as well as to estimate structural system parameters.[16] The frequency-response analysis presented here has been reinterpreted to evaluate disturbance rejection for the cooperative multivehicle-control application. The extension of the frequency-response results to steady-state solutions enables the string-stability analysis for general cooperative control laws that are derived from communication structures. A primary difference in this frequency-response analysis versus the traditional analysis is the inclusion of non-physically representative systems, or non-symmetric stiffness matrices, which does not come without consequences as discussed in the next section.

V. Simulation Results

Simulation results for four different communication structures are presented. The receptance functions and the plots of the steady-state amplitudes and errors are shown to determine the string stability of the cooperative control laws derived from the communication structures. Simulations of ten-vehicle formations are used to verify the frequency-response results, and control-gain design considerations are briefly discussed.

A. Communication Structures

Figure 3 shows the four communication structures that are investigated in this paper. In the figure, vehicle 1 is the platoon lead, which tracks a reference trajectory, and vehicles 2 and 3 are trailing vehicles. These communication structures can be extended to an n-vehicle formation based upon the descriptions in the figure. A fully-connected communication structure means that all vehicles in the formation have information about all of the other vehicles. In communication structure 2, the second through nth vehicles have information about the platoon lead, and the trailing vehicles communicate as described in Figure 3. Communication structures 3 and 4 use a "nearest neighbors" communication approach where vehicles only communicate with adjacent vehicles. The stiffness and forcing matrices for each communication structure are listed in the Appendix. As a result of the control-law development in Section II, the damping matrices are proportional to the stiffness matrices: $C = \beta K$.

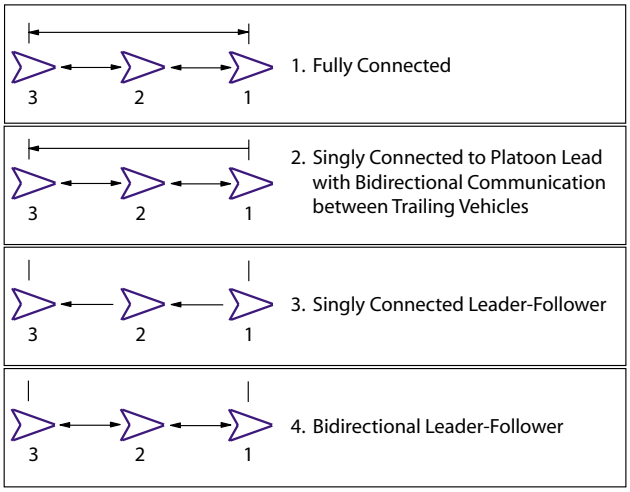

Figure 3. Four possible communication structures for multivehicle formation control.

B. Receptance Functions and Steady-State Errors

The receptance functions and steady-state amplitudes and errors for the communication structures shown in Figure 3 are determined for a ten-vehicle formation. The gains in the stiffness matrices are assumed equal to one; however, communication structure 3 does not yield an invertible Φ matrix for unity gains. The stiffness matrix for communication structure 3 is a lower-diagonal matrix; therefore, the eigenvalues are equal to the

gains along the diagonal. In order to yield n distinct eigenvalues, which guarantees n linearly-independent eigenvectors, the diagonal gains are perturbed. Here, the $k_{j,j+1}$ gains, for $j = 1, ..., n-1$, are perturbed by 0.25 to get $k_{j,j+1} = 1 + 0.25j$. Perturbing the control gains to yield an invertible eigenvector matrix is a consequence of using non-physically representative communication structures. As previously described, the damping matrices are assumed proportional to the stiffness matrices with $\beta = 1$.

Figure 4 shows the receptance functions for the tenth vehicle for the fully-connected communication structure, where $H_{10,k}$ for $k = 1, ..., 10$ is the ratio of the tenth vehicle's output amplitude to the kth vehicle's disturbance amplitude. The receptance functions for communication structure 1 are symmetric due to the symmetry of the stiffness matrix, i.e., $H_{j,k} = H_{k,j}$. Because the control gains in the stiffness matrix are equal, the disturbance effects from vehicles 2 through 10 equally affect vehicle 1. The receptance functions only exhibit one resonant frequency at the first mode, which has a damping ratio of 0.26; the other modes have damping ratios closer to one. Figure 5 shows the steady-state amplitudes (a) and errors (b) for communication structure 1. The plot of the steady-state amplitudes shows that vehicles 2 through 10 have the same steady-state amplitude, and the steady-state errors between vehicles do not grow along the string. Thus, communication structure 1 yields a string-stable cooperative control law.

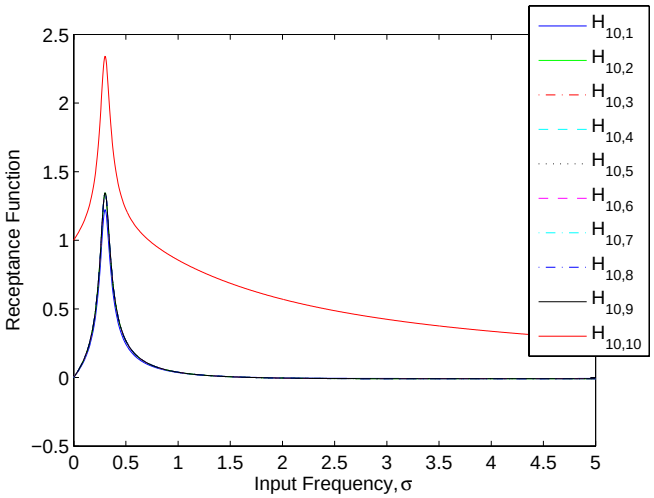

Figure 4. Receptance functions for communication structure 1.

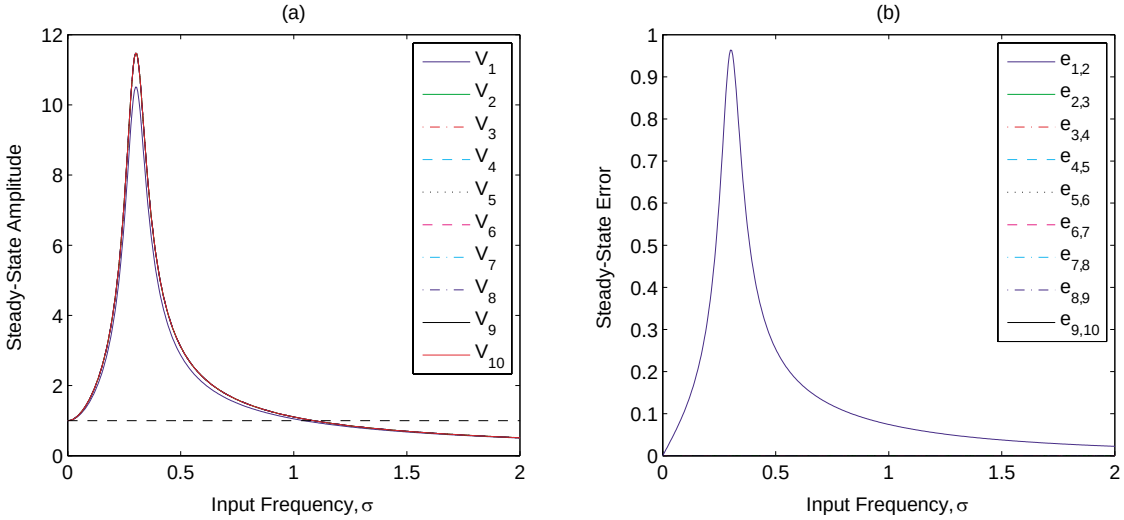

Figure 5. Steady-state amplitudes (a) and steady-state errors (b) for communication structure 1.

The receptance functions and steady-state amplitudes and errors for communication structure 2 are shown in Figures 6 and 7, respectively. In this case, disturbances to vehicles 2 through 9 have unequal effects on the tenth vehicle. The first vehicle has the greatest influence on the tenth vehicle due to its connection to the tenth vehicle as defined by the communication structure. Vehicles 2 through 8 still have an effect on the tenth vehicle even though they are not connected; this shows how disturbance effects can propagate through a vehicle string. The steady-state amplitudes and errors in Figure 7 are similar to those from communication structure 1; therefore, communication structure 2 also yields a string-stable control law.

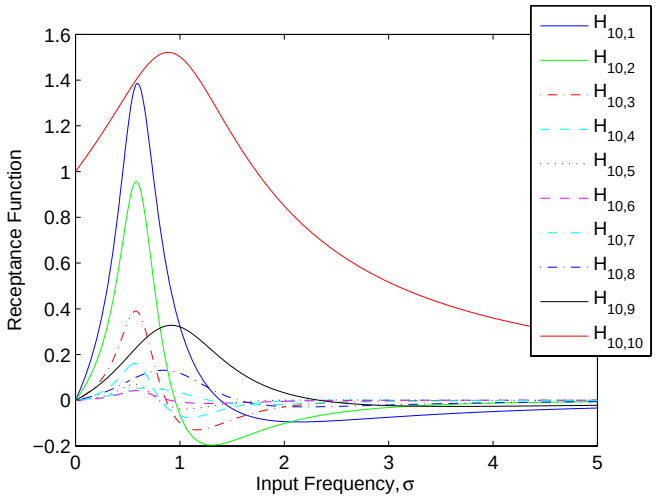

Figure 6. Receptance functions for communication structure 2.

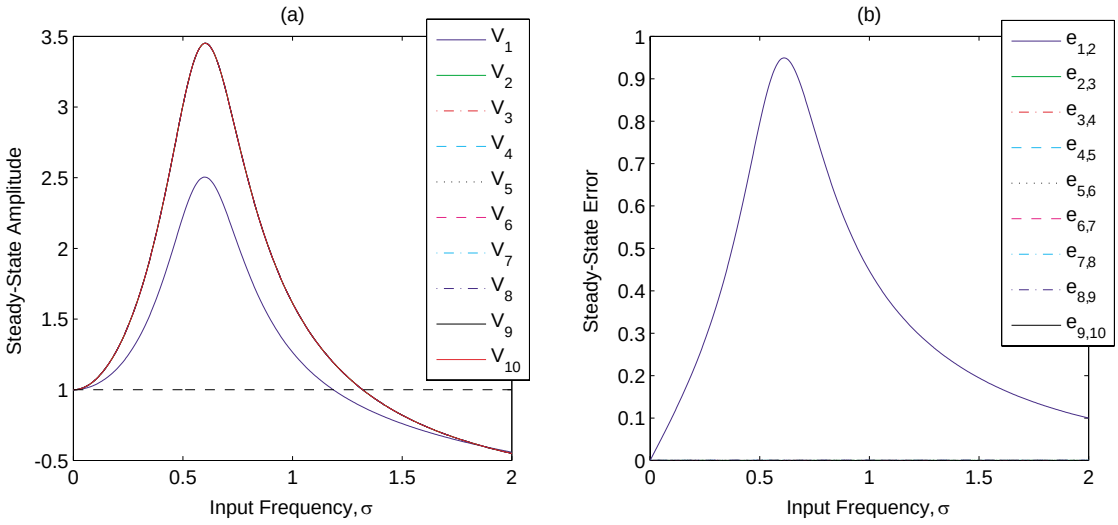

Figure 7. Steady-state amplitudes (a) and steady-state errors (b) for communication structure 2.

The receptance functions for communication structure 3 are shown in Figure 8. For this communication structure, vehicle 10 is connected to vehicle 9 only. However, the peak magnitude of $H_{10,9} < H_{10,8} < ... < H_{10,1}$, which indicates that the disturbance to vehicle 1 has a greater effect on the tenth vehicle than disturbances to vehicle 9. The trends shown in the plot of the receptance functions combined with a priori knowledge of the communication structure indicate that disturbances are amplified along the vehicle string. The plot of steady-state amplitudes and errors in Figure 9 confirm that communication structure 3 is in fact string unstable.

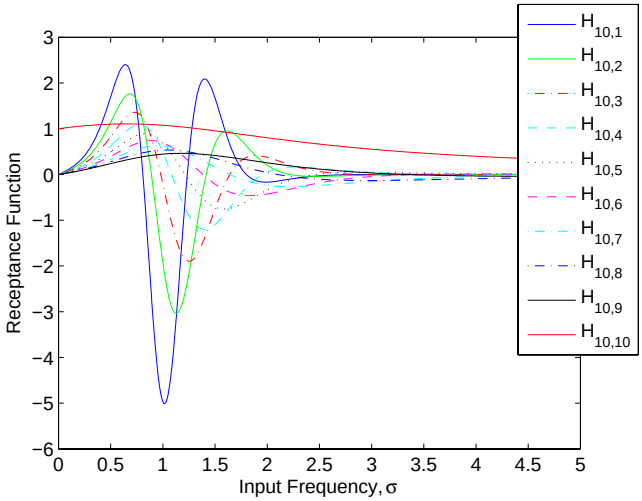

Figure 8. Receptance functions for communication structure 3.

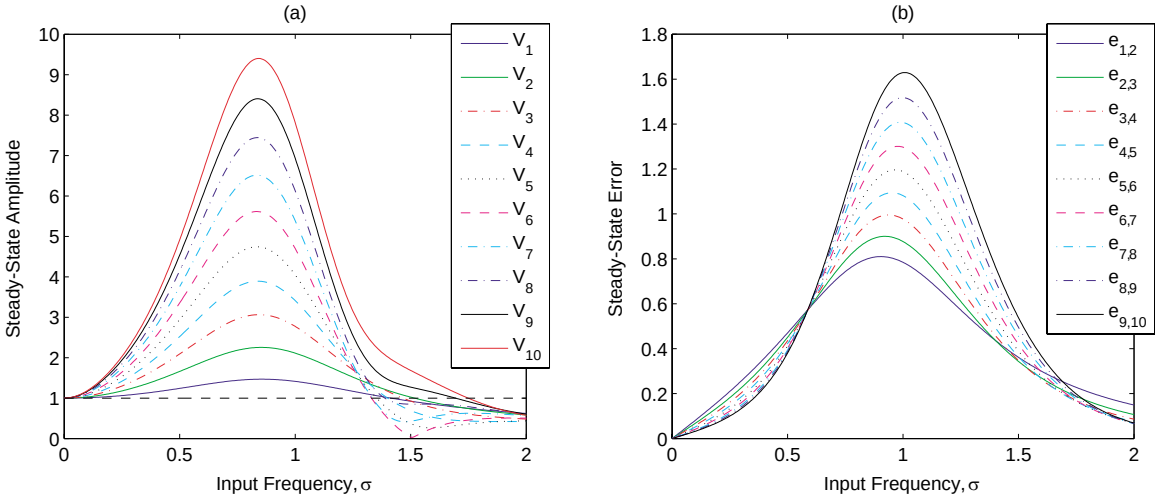

Figure 9. Steady-state amplitudes (a) and steady-state errors (b) for communication structure 3.

Figures 10 and 11 show the receptance functions and steady-state amplitudes and errors for communication structure 4, respectively. Here, disturbances to vehicle 9 have the greatest effect on the tenth vehicle; thus, the behavior of the receptance functions does not indicate string instabilities. A notable difference in behavior compared to communication structures 1 and 2 is evident in the plot of the steady-state amplitudes in Figure 11(a), which shows that the amplitudes increase along the string; however, the steady-state errors in Figure 11(b) indicate that this communication structure does yield string-stable control laws. The growth of amplitudes along the string may be undesirable, but this should be not be confused with string stability, which is defined as the propagation of errors through the string.

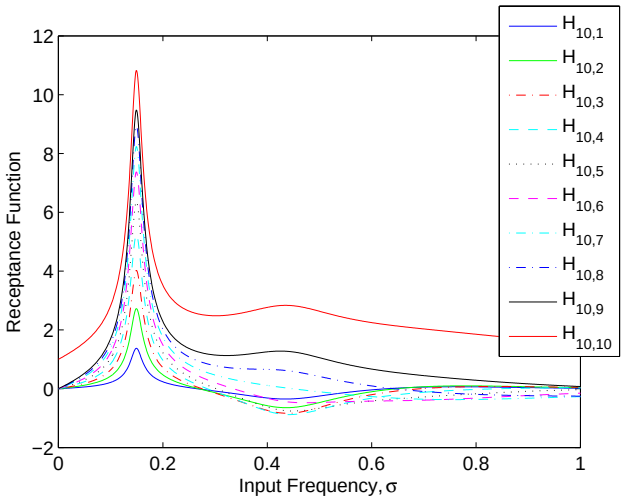

Figure 10. Receptance function for communication structure 4.

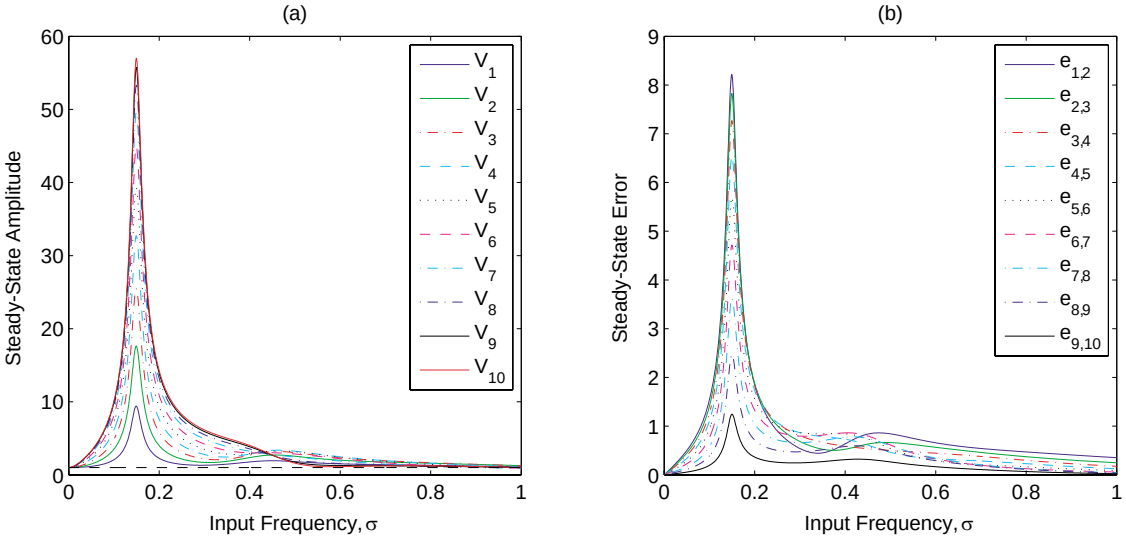

Figure 11. Steady-state amplitudes (a) and steady-state errors (b) for communication structure 4.

C. Formation Simulations

Ten-vehicle formations are simulated for each of the communication structures in Figure 3. The first vehicle in the formation is tracking a constant-velocity reference trajectory in the x direction with $\dot{x}_r = 1$ distance unit (DU) per time unit (TU). Desired separation between vehicles is 1 DU in the x direction and 0 DU in the y direction. Disturbances to each vehicle have the form $d_{x,y} = \cos(\sigma t)$, where σ is equal to the first natural frequency of the system, i.e., the resonant frequency.

Figure 12 shows the simulation results for communication structure 1: spacing errors in the formation in the x direction (a) and control inputs to the vehicle, $\dot{v}$ (b) and ω (c). As predicted by the frequency-response results, the spacing errors in the formation go to zero along the string. In addition, the control inputs to vehicles 2 through 9 are equal. Thus, the simulation results demonstrate that this communication structure yields a string-stable control law with bounded control inputs along the string.

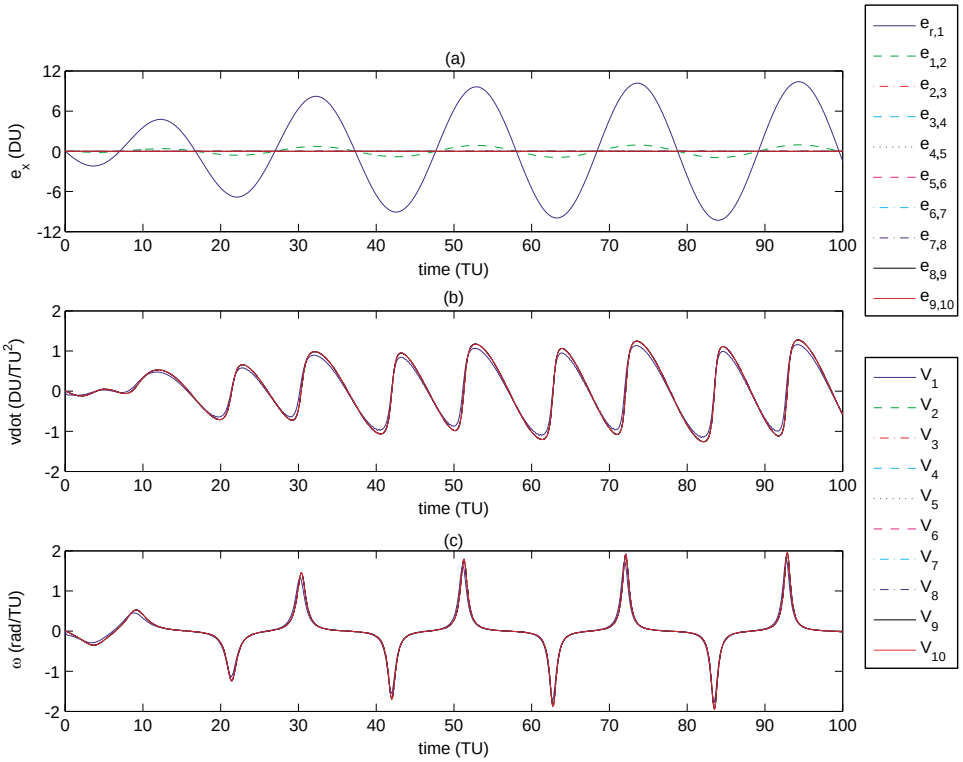

Figure 12. Simulation results for communication structure 1: spacing errors in the x direction (a) and control inputs $\dot{v}$ (b) and ω (c).

Simulation results for communication structure 2 shown in Figure 13 are similar to the results for communication structure 1. Here, the notable difference is the magnitude of the spacing errors, but the control magnitudes are similar.

The frequency-response analysis for communication structure 3 indicates that this communication structure yields string-unstable control laws for the chosen control gains. Simulation results in Figure 14(a) confirm that the spacing errors between vehicle pairs grow along the string as predicted. Figure 14(b) and (c) show the vehicle control inputs necessary to maintain the formation. With the growth of spacing errors along the string, the required control inputs also increase along the string. If these control inputs were bounded, some vehicles in the formation may not be able to maintain their position. Therefore, communication structure 3 would not be feasible for an infinite string of vehicles.

Figure 15(a) shows the spacing errors for communication structure 4. Here, string stability is evident as the spacing errors decrease along the vehicle string. However, the control inputs increase along the string, as shown in Figure 15(b) and (c), which is a result of the increasing steady-state amplitudes along the vehicle string. Compared to communication structure 3, the control inputs are smaller in magnitude, but strings with an infinite number of vehicles would be unable to maintain the formation.

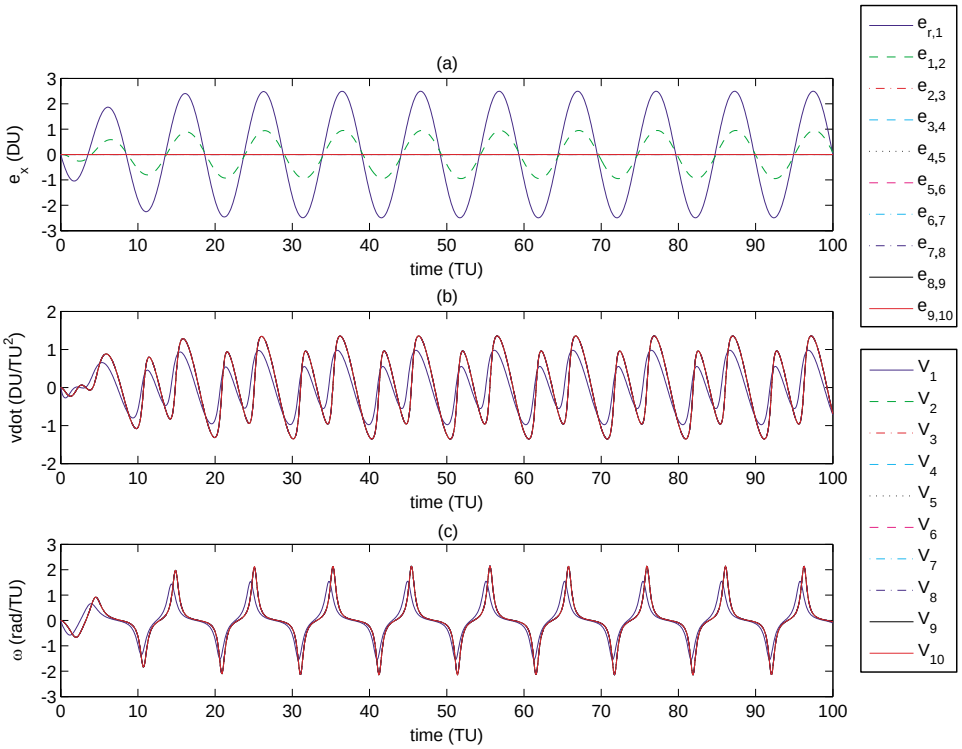

Figure 13. Simulation results for communication structure 2: spacing errors in the x direction (a) and control inputs $\dot{v}$ (b) and ω (c).

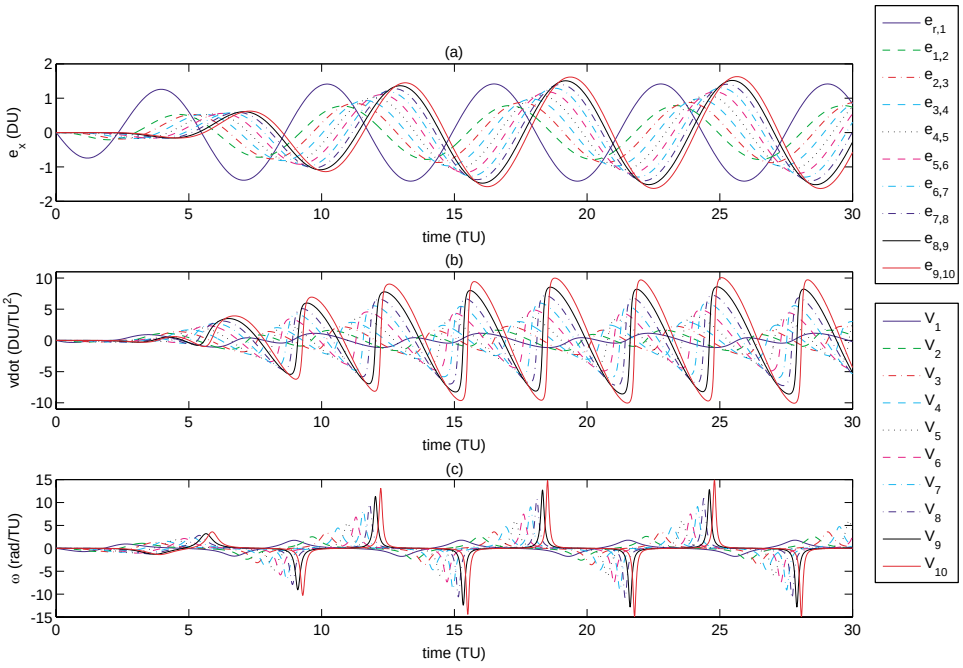

Figure 14. Simulation results for communication structure 3: spacing errors in the x direction (a) and control inputs $\dot{v}$ (b) and ω (c).

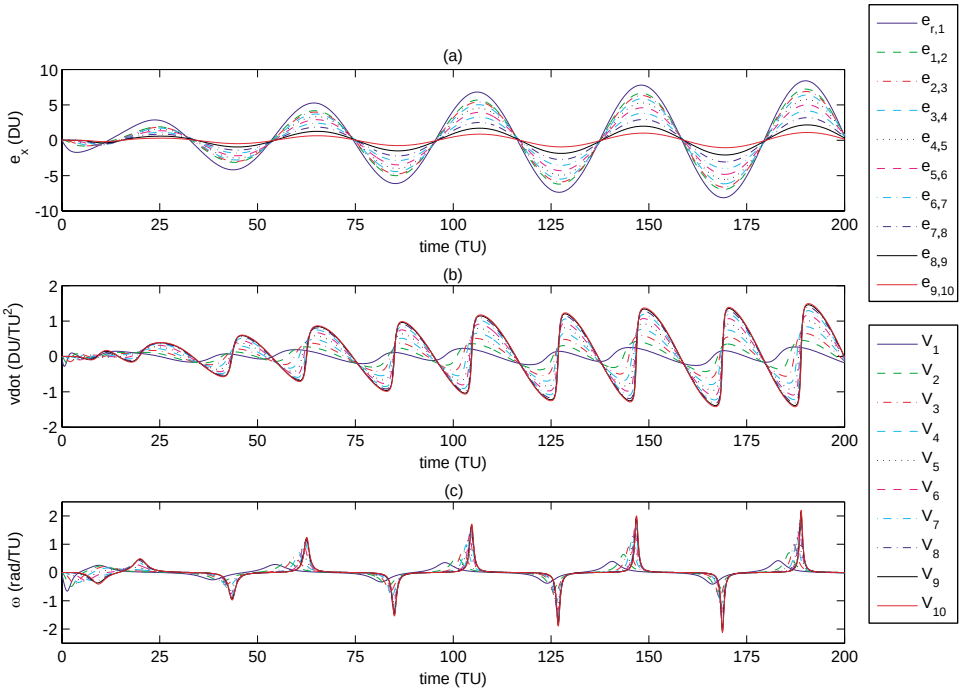

Figure 15. Simulation results for communication structure 4: spacing errors in the x direction (a) and control inputs $\dot{v}$ (b) and ω (c).

D. Design Considerations

The steady-state amplitudes and errors for each communication structure reveal how the multivehicle system will behave when subjected to disturbances. In the simulation cases presented, the nominal gains in the stiffness matrix were equal to one, and the damping matrices were equal to the stiffness matrix. The values of these gains can be changed in order to achieve a more desirable system response.

In the previous section, communication structure 3 was shown to be string unstable for the nominal gain of one. Changing the nominal gain to two, which will be denoted as $k = 2$, decreases the steady-state amplitudes and errors as shown in Figure 16. Figure 16(b) still indicates that the cooperative control laws are not string stable; however, a simulation of the ten-vehicle system shows that the required control efforts to maintain the formation are approximately halved for this gain choice.

Figure 17 shows the steady-state amplitudes and errors for a nominal gain of $k = 1$ with a damping constant $\beta = 2$. Figure 17(b) indicates that this choice of gains leads to a string-stable cooperative control law. Whereas the steady-state errors do not grow along the vehicle string, the steady-state amplitudes still increase along the string. This behavior can be contrasted to the steady-state amplitudes in Figures 5 and 7 for communication structures 1 and 2, respectively. In those cases, the steady-state amplitudes of vehicles 2 through 10 are equal and do not grow along the vehicle string. Communication structures 3 and 4 exhibit similar behavior, which indicates that a connection to the first vehicle in the formation can help to prevent amplitude growth along the string.

The results presented here appear to contradict the string-stability results presented by Swaroop and Hedrick for a preceding-vehicle-tracking control form.[11] Their analysis indicates that a control law using position and velocity errors from the preceding vehicle only is string unstable for all position and velocity control gains greater than zero; in that analysis, all vehicles used control laws with equal gains. However, in the analysis presented here, the perturbations in the gains to permit invertibility of the Φ matrix lead to a string-stable control form. The perturbations were implemented such that the gains increase along the string; and therefore, the trailing vehicles are more aggressive in their control. If the gains are perturbed such that the vehicles are less aggressive along the string, then the string-instabilities remain.

For each design application, the performance objectives and system constraints will help to determine the appropriate control form. String-unstable control forms may be acceptable for a finite number of vehicles in

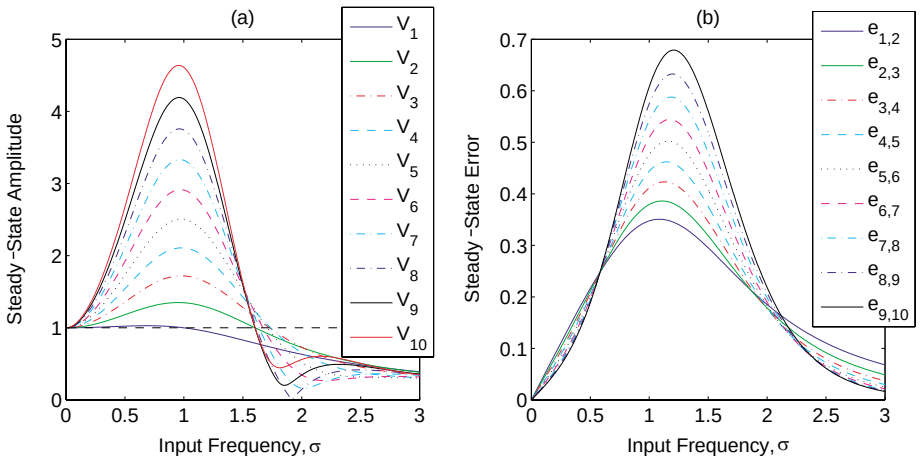

Figure 16. Steady-state amp0itudes of the vehicle positions (a) and steady-state errors (b) for communication structure 5 ($\mathbf{k = 2}$, $\beta = 1$).

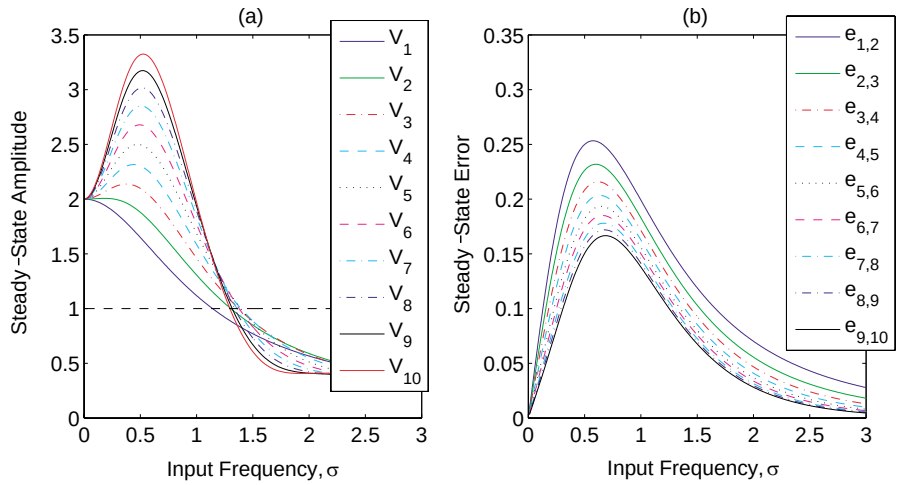

Figure 17. Steady-state amplitudes of the vehicle positions (a) and steady-state errors (b) for communication structure 5 ($\mathbf{k = 1}$, $\beta = 2$).

the formation or string, where control inputs fall within some bounds. As was shown, there is design freedom in the choice of gains. Increasing the gains does not always lead to greater control inputs because the gains may significantly change the way that the system moves as a whole. An obvious drawback to the approach is the need for the Φ matrix to be invertible. Therefore, some communication structures with equal gains cannot be evaluated using this approach.

VI. Conclusions

This paper presents a mechanics-based approach to analyze the string stability of decentralized, cooperative control laws for multivehicle systems. The closed-loop cooperative control laws can be written in a form analogous to structural systems, where the form of the stiffness matrix is derived from an assumed communication structure. Frequency-response functions, interpreted for the multivehicle-control application, are used to evaluate the effect of kinematic-level disturbances on the multivehicle system. The steady-state response of the system is derived from the frequency-response information and is used to determine whether a given control form is string stable. This approach to analyzing disturbances is applicable to general coop-

erative control forms where the closed-loop system can be written in a structural form. One drawback to the approach is the requirement that the matrix of eigenvectors from the stiffness matrix is invertible. Therefore, some stiffness matrices may need to be perturbed in order to yield a full-rank eigenvector matrix; however, it should be noted that perturbations to the control gains do not change the communication structure and trends in the results are consistent as the perturbations go to zero.

The frequency-response analysis was applied to four different communication structures. Whereas the communication structures that include information from the formation lead were shown to be string stable, the communication structure that assumes information from the immediately preceding vehicle only was shown to be string unstable for certain control gains, which was a result shown in the literature. However, this control form was string stable for larger damping gains, which can be attributed to the unequal gains in the stiffness matrix that yield a full-rank eigenvector matrix.

A. Stiffness and Forcing Matrices

The stiffness and forcing matrices are listed for the four defined communication structures in Figure 3. The D matrix acts on the vector $\boldsymbol{u}_r = [x_r(t)\ \dot{x}_r(t)\ d_{r1}\ d_{12}\ d_{13}\ d_{23}]^T$. It is assumed that the first vehicle in the formation tracks a constant-velocity reference trajectory ($\ddot{x}_r = 0$).

1. Fully Connected:

$$K = \begin{bmatrix} k_r + k_{12} + k_{13} & -k_{12} & -k_{13} \\ -k_{12} & k_{12} + k_{23} & -k_{23} \\ -k_{13} & -k_{23} & k_{13} + k_{23} \end{bmatrix}; \quad D = \begin{bmatrix} k_r & c_r & -k_r & k_{12} & k_{13} & 0 \\ 0 & 0 & 0 & -k_{12} & 0 & k_{23} \\ 0 & 0 & 0 & 0 & -k_{13} & -k_{23} \end{bmatrix}$$

2. Singly Connected to Platoon Lead with Bidirectional Communication between Trailing Vehicles:

$$K = \begin{bmatrix} k_r + k_{12} & -k_{12} & 0 \\ -k_{12} & k_{12} + k_{23} & -k_{23} \\ -k_{13} & -k_{23} & k_{13} + k_{23} \end{bmatrix}; \quad D = \begin{bmatrix} k_r & c_r & -k_r & k_{12} & 0 & 0 \\ 0 & 0 & 0 & -k_{12} & 0 & k_{23} \\ 0 & 0 & 0 & 0 & -k_{13} & -k_{23} \end{bmatrix}$$

3. Singly-Connected Leader-Follower

$$K = \begin{bmatrix} k_r & 0 & 0 \\ -k_{12} & k_{12} & 0 \\ 0 & -k_{23} & k_{23} \end{bmatrix}; \quad D = \begin{bmatrix} k_r & c_r & -k_r & 0 & 0 & 0 \\ 0 & 0 & 0 & -k_{12} & 0 & 0 \\ 0 & 0 & 0 & 0 & 0 & -k_{23} \end{bmatrix}$$

4. Bidirectional Leader-Follower

$$K = \begin{bmatrix} k_r + k_{12} & -k_{12} & 0 \\ -k_{12} & k_{12} + k_{23} & -k_{23} \\ 0 & -k_{23} & k_{23} \end{bmatrix}; \quad D = \begin{bmatrix} k_r & c_r & -k_r & k_{12} & 0 & 0 \\ 0 & 0 & 0 & -k_{12} & 0 & k_{23} \\ 0 & 0 & 0 & 0 & 0 & -k_{23} \end{bmatrix}$$

Acknowledgments
Research funding was provided by the NASA Graduate Student Research Program (GSRP) Fellowship.

References

[1]Barmore, B., Abbott, T., and Krishnamurthy, K., "Airborne-Managed Spacing in Multiple Arrival Streams," *24th International Congress of the Aeronautical Sciences*, Yokohama, Japan, September 2004.

[2]Krishnamurthy, K., Barmore, B., Bussink, F., Weitz, L., and Dahlene, L., "Fast-time evaluations of an airborne merging and spacing concept for terminal arrival operations," *Proceedings of the AIAA Guidance, Navigation, and Control Conference*, San Francisco, California, 2005.

[3]Fax, J. A. and Murray, R. M., "Information Flow and Cooperative Control of Vehicle Formations," *IEEE Transactions on Automatic Control*, Vol. 49, No. 9, 2004, pp. 1465–1476.

[4]Stipanović, D. M., İnalhan, G., Teo, R., and Tomlin, C. J., "Decentralized Overlapping Control of a Formation of Unmanned Aerial Vehicles," *Automatica*, Vol. 40, 2004, pp. 1285–1296.

[5]Weitz, L. A., Hurtado, J. E., and Sinclair, A. J., "Decentralized Cooperative-Control Design for Multivehicle Formations," *Journal of Guidance, Control, and Dynamics*, Vol. 31, No. 4, 2008, pp. 970–979.

[6]Jin, Z. and Murrary, R. M., "Stability and Performance Analysis with Double-Graph Model of Vehicle Formations," *Proceedings of the American Control Conference*, 2003, pp. 2223–2228.

[7]Gattami, A. and Murray, R. M., "A Frequency Domain Condition for Stability of Interconnected MIMO Systems," *Proceedings of the American Control Conference*, 2004, pp. 3723–3728.

[8]Yadlapalli, S. K., Darbha, S., and Rajagopal, K. R., "Information Flow and Its Relation to Stability of the Motion of Vehicles in a Rigid Formation," *IEEE Transactions on Automatic Control*, Vol. 51, No. 8, 2006, pp. 1315–1319.

[9]Swaroop, D. and Hedrick, J. K., "Constant Spacing Strategies for Platooning in Automated Highway Systems," *Journal of Dynamic Systems, Measurement, and Control*, Vol. 121, No. 3, 1999, pp. 462–470.

[10]Hedrick, J. K., McMahon, D., Narendran, V., and Swaroop, D., "Longitudinal Vehicle Controller Design for IVHS Systems," *Proceedings of the American Control Conference*, Boston, Massachusetts, 1991.

[11]Swaroop, D. and Rajagopal, K. R., "A Review of Constant Time Headway Policy for Automatic Vehicle Following," *Proceedings of the 2001 IEEE Intelligent Transportation Systems Conference*, Oakland, CA, 2001.

[12]Seiler, P., Pant, A., and Hedrick, K., "Disturbance Propagation in Vehicle Strings," *IEEE Transactions on Automatic Control*, Vol. 49, No. 10, 2004, pp. 1835–1841.

[13]Barooah, P. and Hespanha, J. P., "Error Amplification and Disturbance Propagation in Vehicle Strings with Decentralized Linear Control," *Proceedings of the 44th IEEE Conference on Decision and Control, and the European Control Conference*, Seville, Spain, 2005.

[14]Murray, R. M., Rathinam, M., and Sluis, W., "Differential Flatness of Mechanical Control Systems: A Catalog of Prototype Systems," *Proceedings of the 1995 ASME International Mechanical Engineering Congress and Expo*, San Francisco, CA, 1995.

[15]Hurtado, J. E., *A Kinematics and Kinetics Primer*, Hurtado - Lulu.com, 2008.

[16]Craig, R. R. and Kurdila, A. J., *Fundamentals of Structural Dynamics*, John Wiley & Sons, Inc., Hoboken, New Jersey, 2006.

[17]Junkins, J. L. and Kim, Y., *Introduction to Dynamics and Control of Flexible Structures*, American Institute of Aeronautics and Astronautics, Washington, DC, 1993, Chapter 3.